Tao Zhao · **Gordon G. D. Zhou** · **Qicheng Sun** · **Giovanni B. Crosta** · **Dongri Song**

Slope erosion induced by surges of debris flow: insights from field experiments

Abstract We conducted field observations and experiments to explore debris flow dynamics, sediment transportation and slope erosion at an active natural debris flow gully in the headwaters of Jiangjia Ravine (Dongchuan region, Southwest China). In this region, the hillslopes were heavily jointed, weathered and sparsely vegetated, providing continuous and rich sediment supplies for initiating debris flows. The debris flow propagated in the channel as a sequence of surges, with periodical changes of flow flux, velocity, water content, and viscosity as controlled mainly by the conditions of erodible sediments and water supplies from the upstream. The water content of bank sediments ranged from 5 to 8%, while it was 16 to 26% for debris surges in the channel. The particle size distribution of sediments on the alluvial fan followed the Weibull's cumulative distribution and the mean size was in the range of $2 \sim 4$ mm. The coarse particles were primarily elongated or prismoidal and aspect ratios followed well a normal distribution with the mean value of 0.4. The angular particles entrained in dense viscous debris flow surges could effectively abrade and groove the channel bed and banks, increasing the intensity of slope erosion. The incised slope had a sequence of terraced depositional layers on both banks. The layer thickness decreased as the erosion depth moved deeper into the stratum where hard bed soil/rock layers existed. The water-soil mixture of debris flow exhibited a clear shear-thinning behavior with its viscosity decreasing gradually with the increase of shear rate following the widely accepted power-law model. The dense viscous debris flow can facilitate the transportation of coarse gravels in channel and contribute to slope erosion.

Introduction

Debris flow, as a common destructive geological hazard, can significantly threaten human societies, particularly in mountainous regions due to its high velocity and long runout distance (Cui et al. 2015). It consists of saturated non-plastic debris materials (e.g., sand, clay, gravel, and boulder) with the solid concentration higher than 50% and travelling at velocity of $1 \sim 20$ m/s. A debris flow event can generally be initiated by either the mobilization of landslides or surface water runoff, erosion, and sediment entrainment on hillslopes. In particular, the short duration, moderate to high intensity rainfall is very effective in triggering debris flows (Crosta 1998; Coe et al. 2008; Hungr et al. 2001). As defined by Hungr et al. (2001), an established channel or regular confined path is the key requirement for initiating debris flows as it could effectively carry surface water flow and maintain large flow depth. Debris flow is normally a recurrent phenomenon occurring as a series of surges and separated by flood-like inter-surge flow. The number of surges in a typical debris flow could range from one to several hundred (Hungr et al. 2001; Pierson 1980). In this process, the debris flow front can scour the bed, while the tail reworks the bed by the deposition of soil sediments (Berger et al. 2011; Theule et al. 2015).

The in-channel sediments as an important source of debris mass come from dry raveling of the unsorted colluvial deposits released from the channel banks and the sediments previously mobilized by debris flows surges. The "surged" flow pattern reflects the seasonal variability of sediment production from rockfalls (Loye et al. 2012) and by the episodic colluvial slope failures (Theule et al. 2015). As suggested by Hungr et al. (2005), bed destabilization and erosion, and stream banks failure through undercutting by erosion are two main mechanisms controlling the sediment entrainment in channels. The location of sediment entrainment and magnitudes of the resultant debris flows could be correlated well with the water and sediment supplies, and channel geometries. These entrained debris materials generally do not necessarily have high antecedent moisture levels at debris flow initiation, while they can become saturated during debris flow by runoff (Coe et al. 2008). In this process, soil liquefaction may also develop (Hungr et al. 2001), and the excess pore water pressure in sediments could significantly increase the erodibility of channel bed and the debris flow momentum (Iverson et al. 2011).

The downstream propagation of a debris flow can effectively erode the unconsolidated slope deposits causing the collapsing of its banks. This coupling effect between channel and slope dynamics increases the volume of debris available for being entrained in the debris flow surges. The slope erosion consists of mainly four processes: impact loading, plucking, abrasion, and grooving (Stock and Dietrich 2006), and the intensity is controlled primarily by the lithological characteristics, fluid viscosity, surface runoff intensity and the sediment supply conditions (e.g., grain size, volume, and frequency) (Loye et al. 2012). Field investigations and experiments have revealed that a critical slope inclination angle threshold as low as less than 10° exists for the initiation of debris flows (Denlinger and Iverson 2001; Guthrie et al. 2010; Mangeney et al. 2010). Above this value, a sharp increase of bed scouring by debris flows would occur (Coe et al. 2008). In particular, the debris flow depositional fans are always very susceptible to erosion because of their smooth slope surface, loose soil structure and poorly sorted particle size. The incision depth of a typical flow channel can even reach several meters (Jakob et al. 2005), with a significant geomorphological impact on the local landscape.

The erosion and mass wasting processes of the channel bed and banks can significantly affect the magnitude and frequency of

debris flows, as it contributes effectively to the debris-flow volume (Theule et al. 2015). The volume of entrained sediments has been reported to reach more than 10 times the mass from the source area (Wang et al. 2003), leading to even larger debris flows (McCoy et al. 2012) and changing local morphology of catchment (Sauchyn et al. 1998). McCoy et al. (2012) conducted in situ field tests on debris flow erosions at the catchment scale. They concluded that the near-surface bed sediments would be in a fully dynamic effective-stress fluctuation state during erosion, resulting in a higher potential to be entrained than the deeper sediments. Egashira et al. (2001) studied the entraining characteristics of bed materials into debris flows by flume tests. They concluded that the relative erosion rate of debris flows is inversely related to the sediment grain size. When debris flow occurs in a confined valley, the entrained sediments tend to deposit on steep fans (Crosta and Frattini 2004; Stock et al. 2008). In evaluating the debris volume at any specific channel, the debris recharge rate should also be accounted for (Jakob et al. 2005). The sediment erosions by debris flows could systematically exceeds the depositions, while an equilibrium can be achieved during bedload transport (Theule et al. 2015). As a result, the debris flow can induce large channel deformations, which is effectively influenced by the slope inclination.

Though advancements exist, detailed studies on the mechanisms of slope erosion, flow dynamics and sediment transport by surges of natural debris flow are still limited, due primarily to the episodic occurrence of debris flow and complex field geomorphological settings. In this study, we conducted in situ observations and experiments on slope erosion by debris flow surges at the headwater of a natural debris flow basin at Jiangjia ravine, Southwest China. This study aims to clarify the characteristics of debris flow dynamics and the corresponding mechanical behavior of slope erosion.

Debris flows in the Jiangjia Ravine

As one of the most disastrous debris flow ravines in China, the Jiangjia Ravine is famous for its high annual occurrence of debris flow events (ca. 12 ~ 20 times annually) and huge sediment transportation (ca. 6.91×10^6 t/year) (Hu et al. 2011). It is a tributary to the Xiaojiang River in Dongchuan, Yunnan Province, Southwest China (Fig. 1b), with a drainage area of 48.6 km² and a main channel length of 13.9 km. The relief elevation ranges from 1042 to 3269 m a.s.l. Each year, during the summer monsoonal rainy season, countless slope collapse, landslide and debris flow events occur, which significantly threaten human lives and damage farmlands, houses and infrastructures. In addition, the extremely high sediment yields have markedly reduced the capacity of downstream flood-control and hydro-power generating facilities in Xiaojiang and Jinsha Rivers (Scott and Wang 2004). As stated in Chen et al. (2005), a recurrent cyclical erosion/deposition morphodynamic behavior was observed in the lower reach of Jiangjia Ravine, which severely changed the morphology of channel bed. During the rainy season (from May to September), the change in height and width of the channel section can reach several meters after a debris flow event.

In this research, a small active debris flow channel at Menqian Gully was identified during a field trip in July 2017 as a testing site, as shown in Fig. 1c. In particular, on the low relief hillslopes, sparse vegetated terraces were recognized, while the upper reach
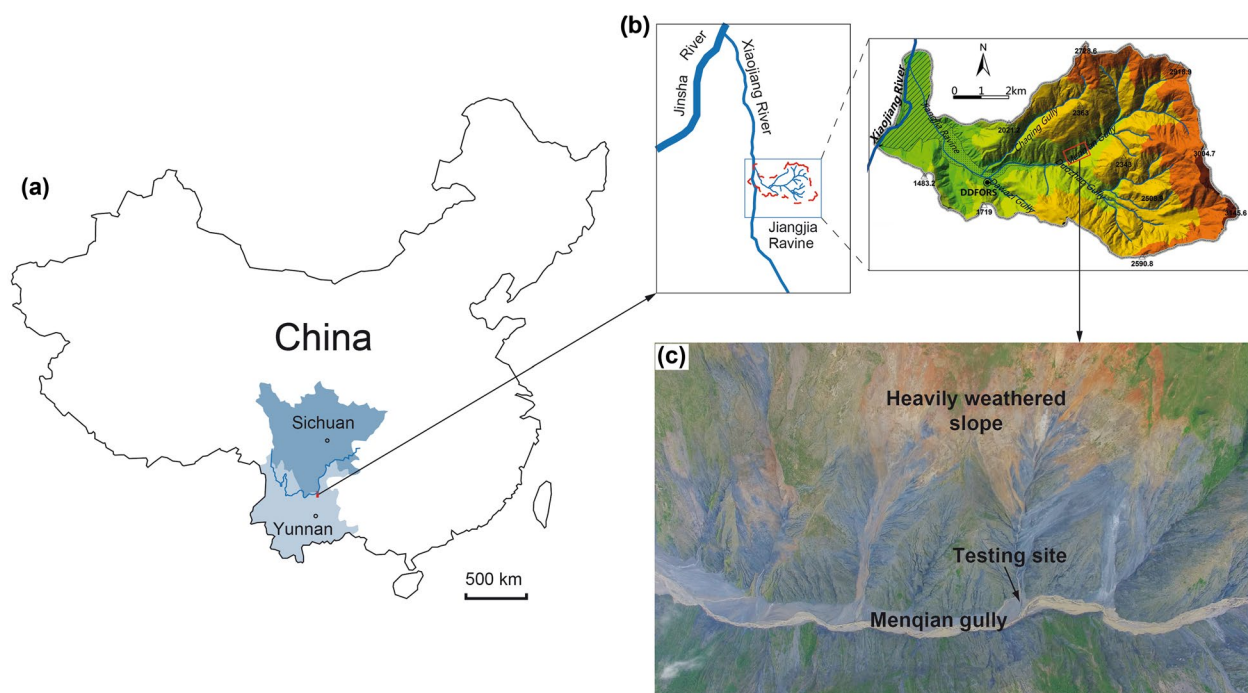

Fig. 1 **a** The location of the Jiangjia Ravine in the Southwest China. **b** The Jiangjia Ravine (modified after Zhou et al. (2019)). In **b**, DDFROS: Dongchuan Debris Flow Research and Observation Station. **c** Aerial view of the Menqian Gully and the debris flow observation and testing site

Fig. 2 **a** Aerial view of the field observation and experimental site. In **a**, A: the debris supply zone; B: debris deposition fan; C: a small creek in the Menqian gully. **b** A photo of the experimental site with a sequence of incision terraces. In **b**, D: an active debris flow surge; E: sediment terrace formed by antecedent debris flow surges. **c** A photo of the downstream debris flow deposition fan and creek at location "C" in **a**. The direction of the active debris flow is marked by an arrow
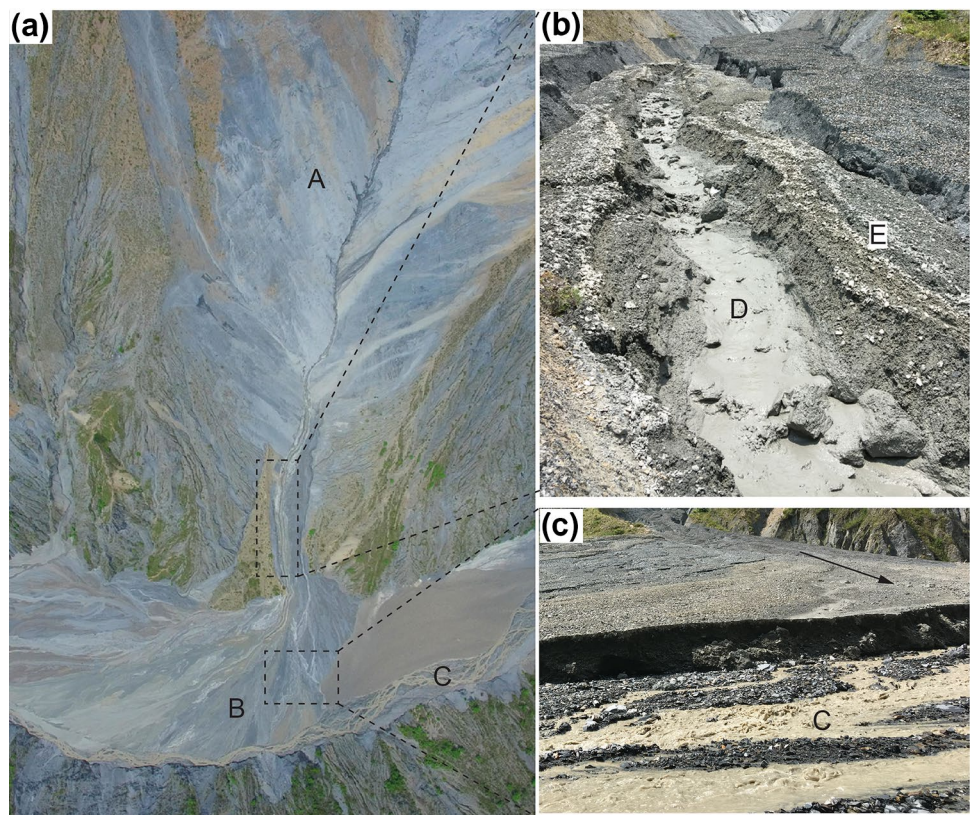
at an elevation of around 1800–2300 m a.s.l. was heavily weathered with almost no vegetation. Sandy-clayey colluvium was widely observed on the talus slopes.

The study area is a second order drainage channel (see Fig. 2a). The local heavily weathered and sparsely vegetated hillslopes in part because of progressive long-term deforestation in history are affected by large and frequent landslides and debris flows. The thick, unconsolidated, poorly sorted and matrix supported colluvium deposits form an apron downslope and are prone to intense gullying and landslides resulted from the surface water runoff and debris flows due to their relatively low strength and weak internal structures (see Fig. 2b). The mean particle size (d_{50}) of samples collected from the debris deposition fan (see Fig. 2c) is in the range of 2 ~ 4 mm (Zhou et al. 2019). Using the dynamic image analysis technique (Wei et al. 2020), the aspect ratio of coarse particle (size > 1 mm) can be quantitatively analyzed. As shown in Fig. 3, the particle aspect ratio follows well a normal distribution, with the mean value of 0.4. The distribution pattern indicates that debris particles in the gully are primarily elongated or prismoidal, which are favored by debris erosion due to their sharp edges and high apparent frictions.

As observed by Scott and Wang (2004), the sediments in the channel came mainly from the gradual mobilization or flushing of the debris deposits accumulated in the gully by various mechanisms, such as small landslides, dry sliding, wet creep in the summer, and bank erosion of previous deposits since the last few flow events. During the field observations, no debris flow mobilized from local landslides has been observed, indicating that the active debris flows in the channel were initiated mainly by the sediment entrainment.

Since no rainfall occurred at the time of field trip, the water supply was mainly from the surface water flow and underground seepage in the upslope. The debris flow propagates in the channel as a series of surges, the volume and frequency of which depend mainly on the sediment and water supplies from the upper reaches of the channel. This type of "surged" flow has also been widely observed
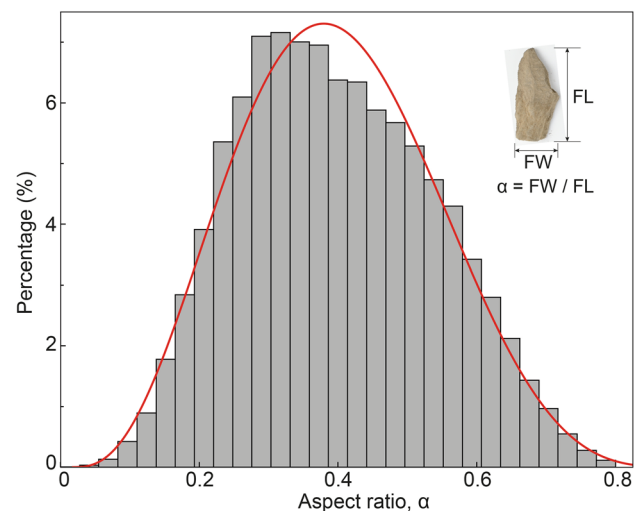

Fig. 3 Statistics of the aspect ratio for 243,741 particles of size 1–10 mm collected in Menqian Gully. The statistical analysis was performed by the PartAn3D Maxi particle size and shape analyzer (Microtrac 2021)

by other researchers in the field, which reflects the pulses of sediment supplies from the upper catchments (Coe et al. 2008; Theule et al. 2015). Between successive flow surges, the debris flow may completely cease motion and the flow channel would retain a significant volume of debris mass. We also observed that sediments in the channel can be temporarily depleted after a major debris flow flushing, and then refilled by subsequent surges (see Fig. 2b). The recurrent debris flow events in this channel have produced a

well-defined elongated debris depositional fan, as shown in Fig. 2c. The toe of the fan has extended into a small creek in the Mengqian Gully (e.g., location "C" in Fig. 2a, c), which was continuously eroded by the stream flow. As stated in Hungr et al. (2001), the toe erosion process could effectively unload the deposition and enhance the mobility of further downslope sediment movement.

Figure 4a shows the active debris flow gully and an antecedent dry gully. The active gully was formed after a recent debris flow
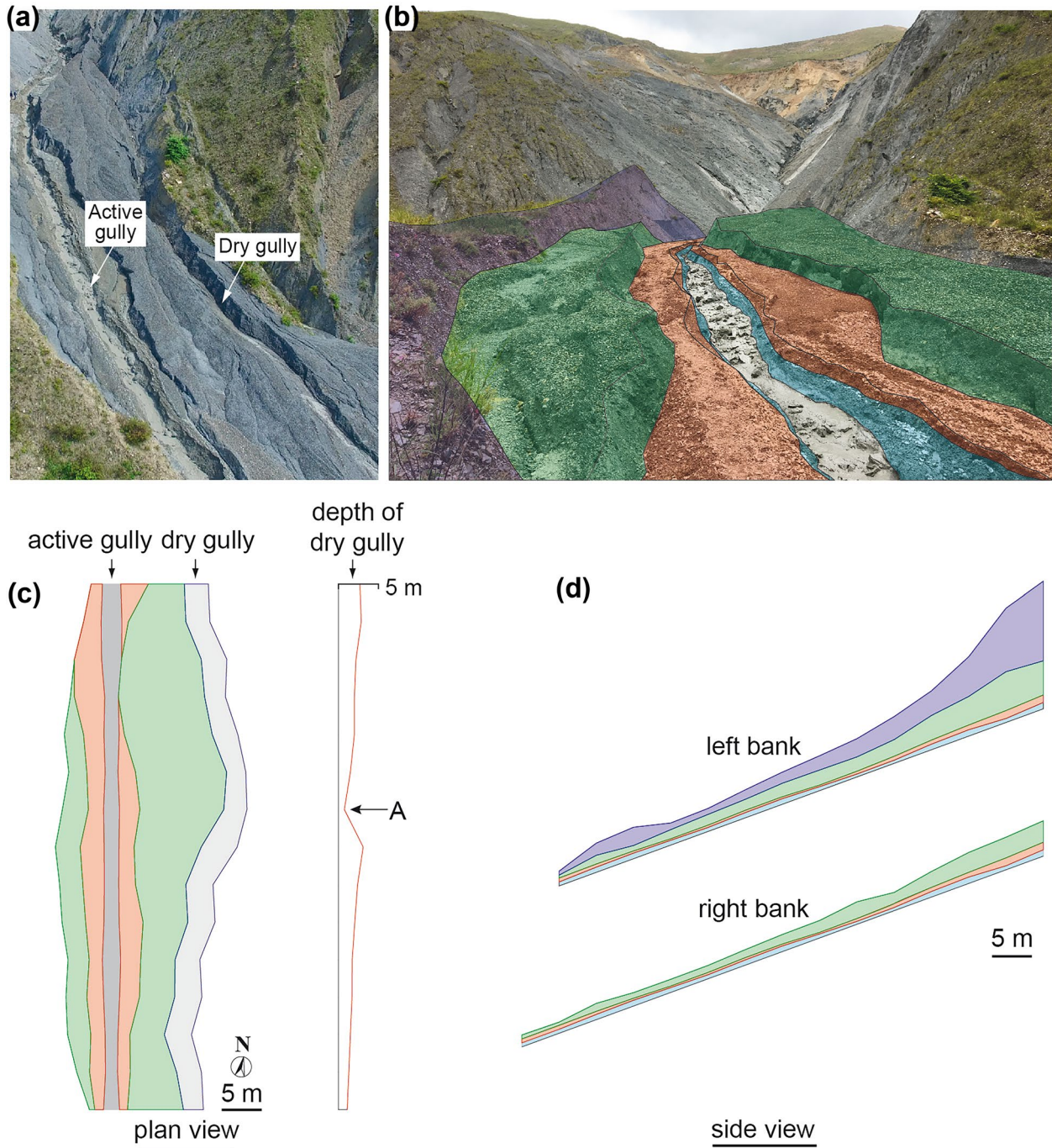

Fig. 4 a An aerial view of the field observation and experimental site. **b** Sediment deposition terraces resulted from erosions by a sequence of surged debris flows. **c** A sketch of the debris deposi-

tion zone, with the coeval debris flow levees colored the same. **d** Sketches of the left and right banks of the channel

diversion. The colluvium adjacent to channels has been intensely undercut by erosion, forming oversteepened vertical or subvertical channel banks which could consistently supply debris materials to the channel by raveling and small landslides. The adequate sediment supply also explains why the debris flow surges could occur continuously in sequence over short time frames in the gully. In the antecedent dry gully, the channel bottom was found to be made of highly consolidated sediments and intact bedrock, which could effectively resist erosion by debris flows. As both the active and older gullies are situated on the same alluvial fan, the channel depth of the dry gully in Fig. 4c is considered as the maximum scouring depth the active debris flow gully could reach.

As shown in Fig. 4a, the channel has a complex morphology combining both erosional and depositional forms, resulting from debris flow erosion and replenishment in a series of surges. The strips of the same color in Fig. 4b–d illustrate the coeval debris flow levees which were then incised by subsequent debris flow surges. According to the field recognition, the incision and avulsions by debris flows have led to the lateral migration of debris depositions over time. The gradual decrease of gully depth in the up and downstream of location "A" in Fig. 4c was likely due to the flow obstruction by a huge boulder embedded in the middle section of the channel. The side views of the left and right banks of the active gully are illustrated in Fig. 4d. During the visits to the site for two successive days, the channel width and depth increased significantly after a light rain overnight, showing that the channel could quickly fill and expand through the erosion of channel banks.

Field experiments of slope erosion by debris flow surges

To investigate the dynamics of debris flow and slope erosion, a relatively gentle section (~15°) of the active gully in Fig. 4a was selected as the observation and experimental site (see Fig. 5a). A small sediment slope was piled up in the channel using the loose sediments at both banks during the interval (~20 min) of two surges when the debris flow was stationary in the channel (see Fig. 5b). Gentle compaction was applied on the slope to reproduce the in-situ stress state of the loose debris deposits. Due to the limited access to accurate surveying tools in this remote site, tree branches and steel posts were installed at 0.6 m away from the slope center in the upstream and downstream sections of the channel to measure the width and height of debris flow during the tests, as shown in Fig. 5b, c. Two monitoring locations at 10 m (location "4" in Fig. 5a) and 5 m (location "2" in Fig. 5a) away from the piled slope in the upstream and downstream sections were selected, respectively. After the stationary interval, a sequence of debris flows surged downstream, impacting and eroding the slope. During the field experiments, a number of tracing foam blocks were placed at the surface of the flow to measure the mean flow velocity.

As observed in the field, the debris flow moved as a slurry mixture of water, soil, and rock fragments. It exhibited periodically
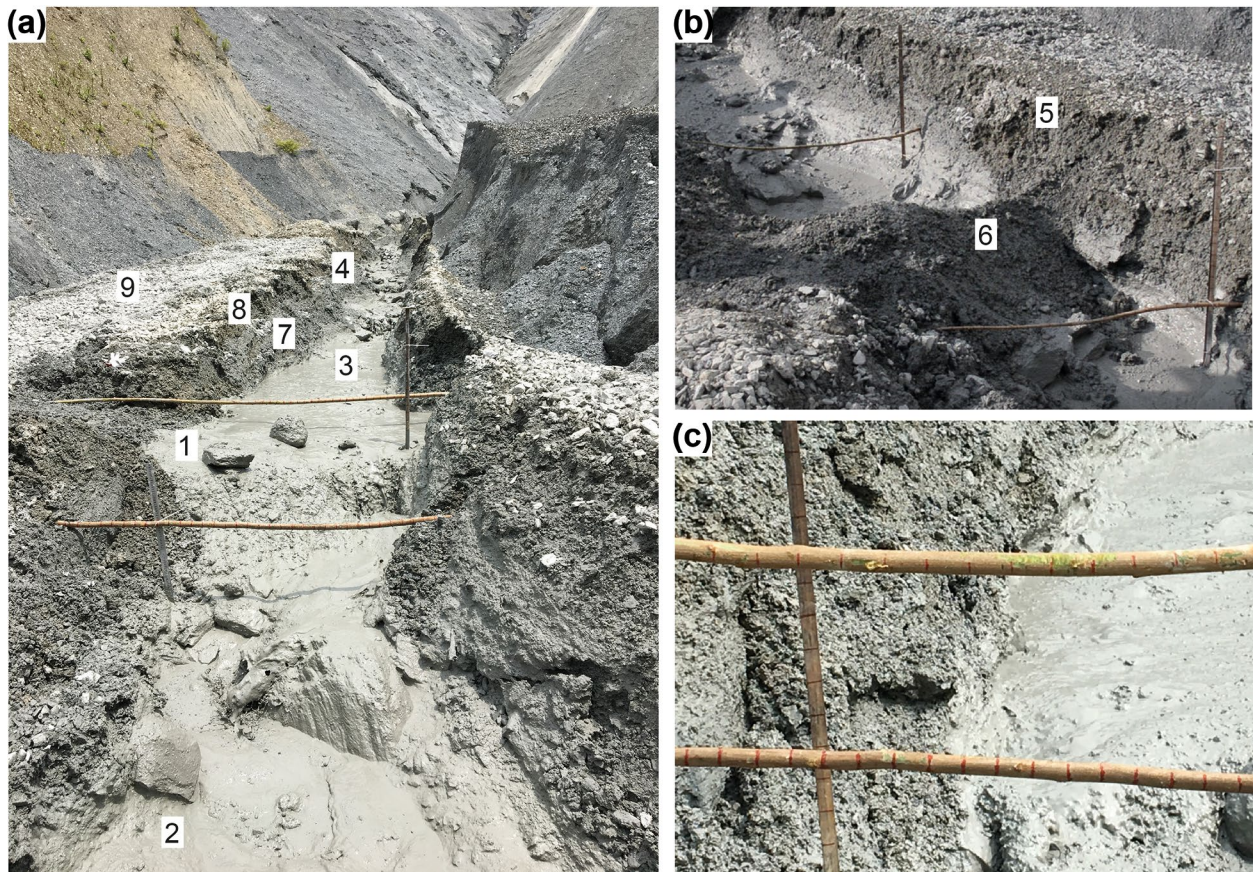

Fig. 5 Configurations of the experimental site. **a** Overview of the site. Numbers 1–9 are sampling locations. **b** An artificial earth dam piled up at the site. **c** Detailed view of the horizontal and vertical measurements. The interval of the measurement ticks is 10 cm

Table 1 Soil/slurry properties at various locations of the observation site. Data unavailable is marked as "-"

Sampling location	1	2	3	4	5	6	7	8	9
Water content, w (%)	16.4	17.3	25.8	7.9	7.8	7.7	8.6	5.4	2.1
Density (g/cm³)	2.1	2.26	1.97	2.23	2.31	2.29	-	-	-
Slurry density (g/cm³)	1.68	1.74	1.44	-	-	-	-	-	-

different flow rheology, ranging from the dilute water-laden slurry to extremely high viscous flows. This is controlled mainly by the water supply from the upstream and soil concentration in the flow. The debris samples were collected from the gully and the slope, and then tested for material density, water content and viscosity at the Dongchuan Debris Flow Research and Observation Station (DDF-ROS). The results are summarized in Table 1. The shear strength parameters of sediments at location "6" were tested by the direct shear tests, with the cohesion of 11 kPa and the internal friction angle of 35°. The grading curves of samples collected at locations "4" and "6" are shown in Fig. 6, which can be best fitted by the Weibull's cumulative distribution function (WeibullCDF).

The testing results of slurry viscosity are shown in Fig. 7 which exhibit a clear shear-thinning behavior with gradually decreasing values as the shear strain rate increases. In addition, the slurry viscosity decreases with the increase of water content in the slurry. The results can explain the phenomenon that dense viscous debris flows exist at low flow rates, while very dilute water-rich debris flows exist at high flow rates as observed at this site. On a logarithmic scale plot, the results can be fitted by the most widely used power-law model for non-Newtonian fluid (Bird 1976) as

$$\mu = m\dot{\gamma}^{n-1} \tag{1}$$

where m and n are fluid consistency coefficient and the power-law index, respectively. m corresponds to the viscosity at the shear rate of $1\ s^{-1}$ and $n < 1$ for a shear thinning liquid.
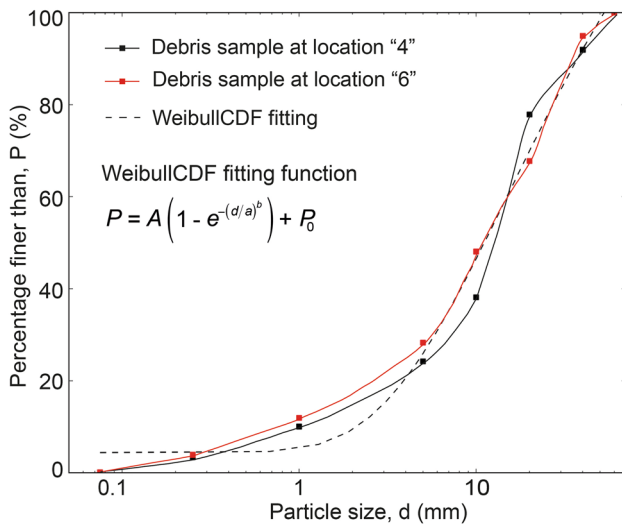
The erosion of the artificially piled up sediment slope by surges of debris flow is shown in Fig. 8. At time (b) 00:07, the debris flow first arrived at the slope and then gradually increased in height as it was retained by the slope. The flow velocity at that moment was 1.25 m/s. At time (d) 01:18, the debris slurry reached the slope crest and started to overtop the right bank of the slope. The occurrence of outburst on the right bank resulted from the main flow stream direction towards the right-hand side. Clear surface water runoff and wet zone was observed on the downstream side of the slope. The saturated (wetting) region enlarged gradually as more incoming debris slurry from the upstream accumulated in the channel. At (g) 01:47, the debris flow started to overtop the middle section of the slope. The velocity of surface flow was initially very slow as 0.5 m/s with small volume of overtopping materials. It increased quickly as the supply of debris slurry increased in the channel and the flow elevation dropped suddenly. Thus, intense erosion of sediments at the downslope surface occurred, as indicated by the appearance and gradual enlargement of the flow gully on the downstream surface of the slope. At (h) 02:33, the bottom region of the right slope (the region enclosed by the red dashed line) collapsed and then was washed away by the flow. At (i) 02:48, two medium sized boulders, around 30 cm in size, blocked the middle gully on the slope crest, which was shortly washed away at (j) 03:00 by the incoming debris flow. The continuous supply of debris slurry from the upstream also increased the rate of debris flow erosion on the slope. At (k) 03:07, a second slope collapse occurred near the right bank and a new surface flow gully appeared afterwards at the right-hand side of the slope. At that moment, the downstream flow
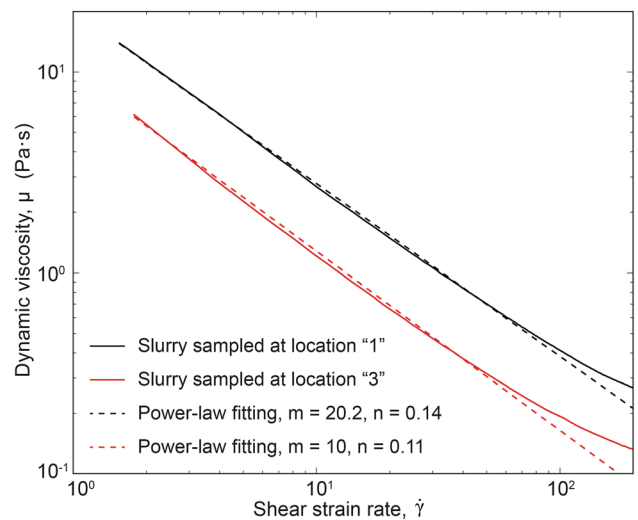

Fig. 6 The particle size distribution of samples at locations "4" and "6." The fitting parameters: $A = -138.7$, $a = 12.97$, $b = -0.68$, $P_0 = 143.3$

Fig. 7 The slurry viscosity tested by the rheometer Physica MCR301 (AntonPaar 2021). The dashed curves are fitting lines by Eq. (1)
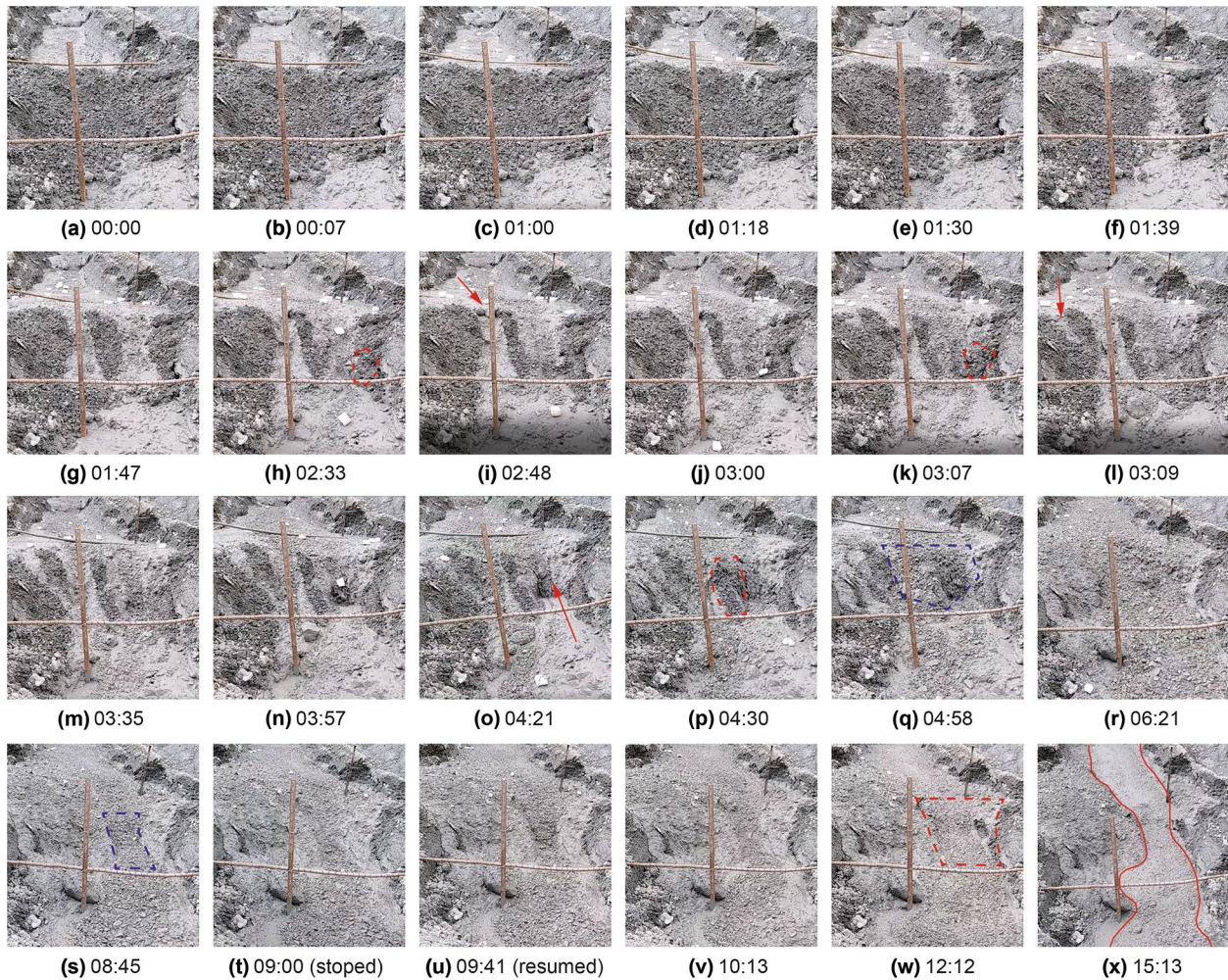
Fig. 8 Snapshots of the debris flow in the gully from the field filmed video. The time below each plot is the video recording time from the start of the test (unit: minute:second). The start of the test is defined as the debris flow surge approaches the upstream monitoring location which is 10 m from the testing site. The red dashed polygons in (h), (k), and (p) indicate the collapsing zones. The blue dashed polygons in (q) and (s) indicate the temporary with of the incised gully, while the red dashed polygon in (w) indicate the final incised gully on the slope

velocity was measured as 0.8 m/s. At (o) 04:21, part of the middle slope ridge collapsed, widening the right gully significantly. At (p) 04:30, the middle and right flow gullies merged into a larger gully of the width 1.8 m, which boosted the erosion of debris flow. This large gully stream persisted for around 4 min and the flow velocity remained relatively high. At (q) 04:58, the whole slope was washed away by the debris flow. The backward erosion dominated in the middle and right sections forming the mainstream of flow, while the left section gradually dried up. After that, the debris flow velocity decreased gradually, and it stopped completely at (t) 09:00. At (r) 06:21, a large boulder block (of diameter ~ 40 cm) was stopped by the measurement post and then deposited at the left-hand side of slope toe. It served as a key rigid block stopping the backward scouring of the flow and protecting the left slope from collapsing. After 41 s (u), the in-channel flow resumed, but the velocity was still very low (< 0.3 m/s). The debris flow surge stopped and resumed periodically between (u) and (w), at much reduced time

interval. At (w) 12:12, a deeply incised gully formed on the right-hand side of the channel and then the flow shifted to the right-hand side (x).

The evolution of debris flow velocity and flow width are illustrated in Fig. 9. In the test, the time (t) used for the debris flow to move from the upstream to downstream reference points, i.e., the distance between the two steel posts (1.2 m), were recorded. Then, the debris flow runoff velocity was calculated as the ratio of moving distance to time. The flow width was measured at the slope crest before the collapse of the slope, while the channel width was measured when a large gully was formed. The measured data were all obtained from the post-analysis of the field recorded video (see the complementary information of this paper). As shown in Fig. 9a, the debris flow started to overtop the slope at 84 s. The initial surface runoff velocity was 0.15 m/s, and the breaching width of the slope was 0.25 m. As more debris materials from the upstream reached the slope, the runoff velocity increased quickly. It fluctuated slightly

Fig. 9 Evolution of **a** debris flow runoff velocity and **b** flow width. In **b**, the constant width period between 530 and 790 s represent the width of channel bottom section
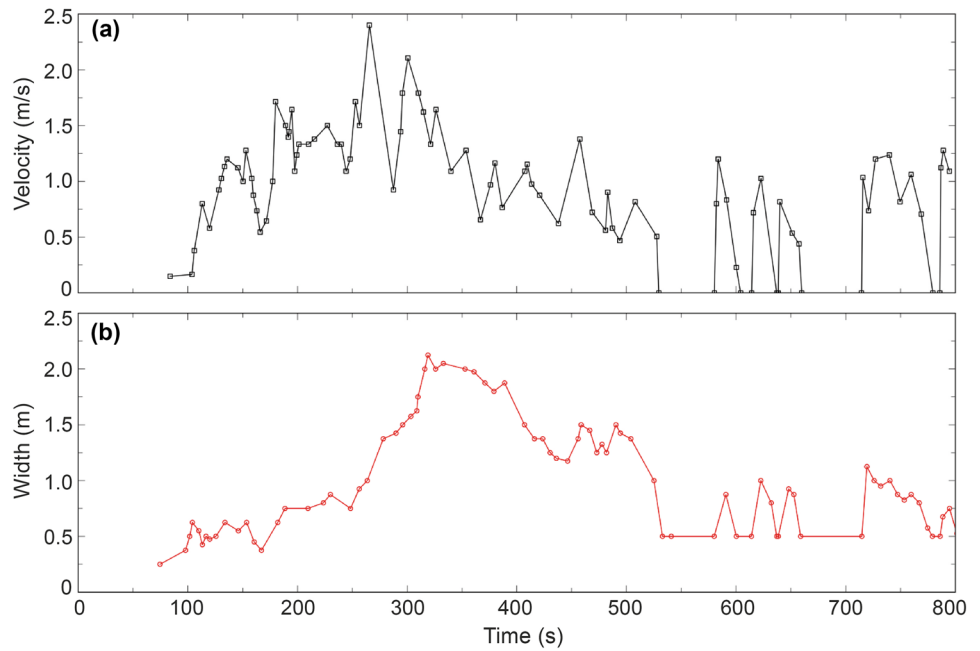
when the channel width increased because of surface erosion. The erosion can effectively entrain and wash away the surface sediments, resulting in a gradually deepened gully. Correspondingly, the channel width increased gradually. After 500 s, the debris flow surge stopped and resumed periodically, as reflected by the varied flow velocity and channel width. Meanwhile, the channel width changed little, indicating that the channel could maintain stable, and the debris flow could hardly erode the hard slope bedrock/soil layers.

Discussion

Transportation of coarse gravels by debris flow

The debris flows have been reported to be able to transport coarse gravels and even huge boulders to a long distance (Scott and Wang 2004). They can exhibit apparent viscous behavior, similar to wet cement. The viscosity has been reported at over 1000 times that of pure water at 20 °C (Pierson 1980). As a result, the debris flow can effectively transport large boulders of size larger than 10 cm "floating" at the flow surface (see Fig. 10a). This process can be further enhanced by the "rough sorting" process, bringing the large rock clasts to the flow surface and flow front (Costa 1984). During the site observations, coarse gravels have been widely found in the upper layer (see Fig. 10b) and surface (see Fig. 10c) of the debris deposits.

According to the field observation, an appreciable portion of clay was found in the debris sediments. After mixing with water, these clay particles can form a clay slurry, which can be very viscous and thick at the static state, but thin out when agitated (i.e., the thixotropy phenomenon). As a result, the debris flow exhibits a strong non-Newtonian fluid behavior. Theoretically, the settling of a single particle in a non-Newtonian shear-thinning liquid is governed by the modified Stokes drag law (Ceylan et al. 1999; Chhabra 2007), as

$$F_d = \frac{1}{2}C_d\rho_f V_r^2 A_P \tag{2}$$

where C_d is the drag coefficient; ρ_f is the fluid density; V_r is the relative settling velocity; A_p is the projected area of the particle. The drag coefficient can be expressed as,

$$C_d = 24Y_n/\text{Re}_n \tag{3}$$

where Y_n is the drag correction factor as a function of n ($Y_1 = 1$). There are various forms of drag correction factor such as $Y_n = 3^{n-1}$, $Y_n = (0.832)^{(n-1)/2}$, while there is no consistent agreement on the general expression in the literature. Re_n is the modified Reynolds number as

$$\text{Re}_n = \rho_f V_r^{2-n} d^n/m \tag{4}$$

where d is the effective particle size; m, n are parameters as defined in Eq. (1).

As shown in Eq. (3), the drag coefficient, C_d, decreases with the increase of Re_n. For a debris flow of high shear rate (e.g., high flow velocity along the channel), the fluid viscosity is low (Eq. (1)). Thus, the settling velocity (V_r) should increase to maintain the force balance, leading to rapid deposition of coarse grains. Thus, the debris flow would become dilute. This process also reduces the overall density of the slurry because of the cascading change of solid concentrations in water. According to fluid dynamics, for channel flows with non-slip boundary condition, high shear rates exist near the lateral and bottom boundaries, such that the slurry viscosity decreases significantly there. This would lead to the rapid settling of coarse grains and consequently the decrease of overall slurry density near the lateral slope banks. Thus, the slurry near both banks was always dilute, while the middle stream flow could remain in a dense state transporting the major portion of coarse gravels (see Fig. 10a).
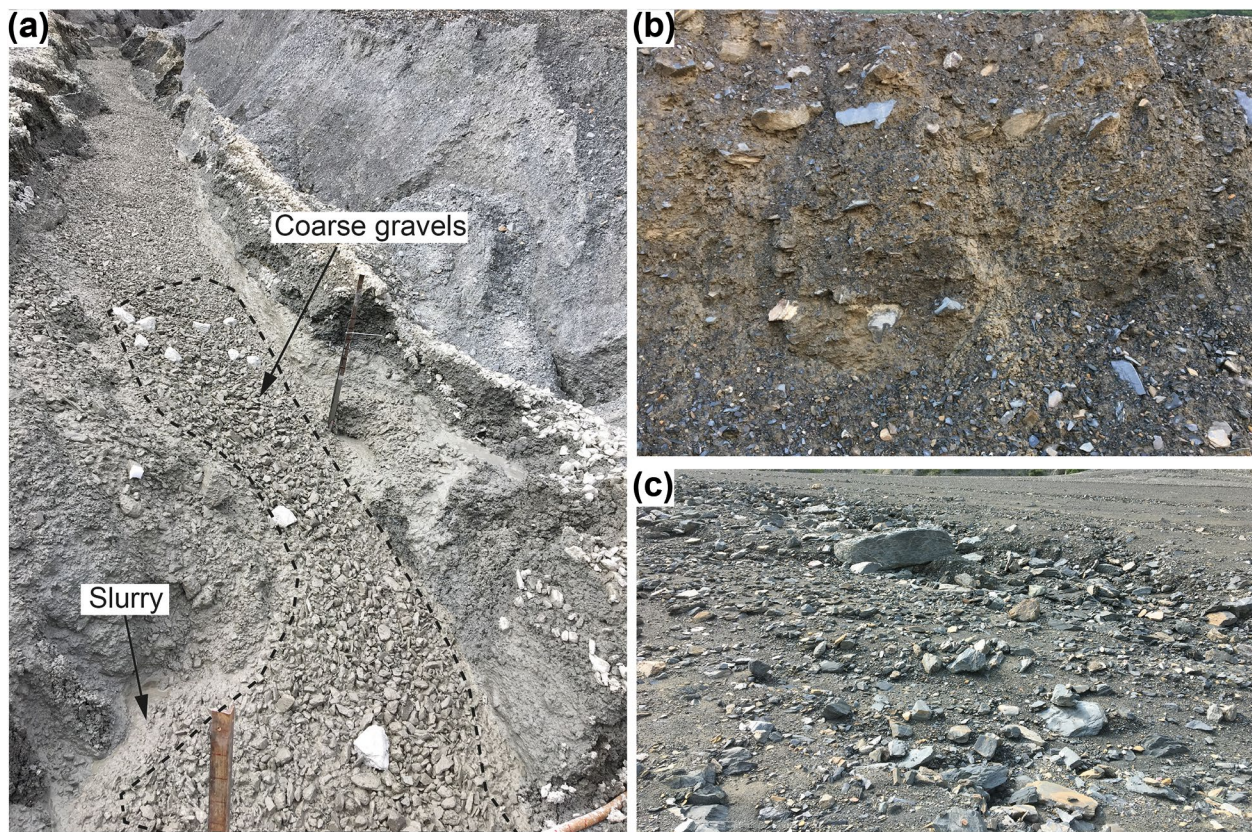
Fig. 10 Evidence of coarse gravel transported by debris flows. **a** An active natural debris flow gully (note: the large white boulders were thrown into the channel from the left bank of the gully). **b** A sub-vertical section of a debris deposit fan. **c** Dry surface debris deposits in the Menqian Gully

Slope erosion by surges of debris flow

The multiple debris flow surges observed in the field experiments can be explained by the flow instability, which causes uniform flows to evolve into a series of waves (Davies 1986). The surges form as continuous inflow of debris materials from the upstream into downstream reaches. The downstream reaches are generally wider and less steep, and already contain a large volume of static debris deposits. The incoming flow would slow down when it reaches the downstream region and then pile up on these existing static deposits. As stated in Hungr et al. (2001), the thrusting or overriding of debris materials would increase the total stress causing a concomitant increase of pore water pressure. This process could result in enhanced acceleration of debris flow, delivering more fresh sediments to the downslope regions. At some critical state, the accumulation of inflow debris materials would finally trigger the discharge of a surge, temporarily depleting the reaches.

As the debris flow propagates downstream in the channel, the angular rock fragments entrained in the saturated surges could abrade and groove the bed and bank sediments intensely (Stock and Dietrich 2006). These coarse rock clasts are primarily elongated of relatively low aspect ratios (Fig. 3) and widely distributed on the talus slope (Fig. 2b) and in the channel (Fig. 10a). As illustrated in the site experiments in Fig. 8, the presence of coarse gravels in debris flows could effectively boost the intensity of slope erosion. This effect was

particularly evident on the dam downslope surface where the flow velocity was high. In addition, the water content in sediments also plays an important role in controlling the soil strength and thus the efficiency of debris flow erosion (Huang et al. 2002; Matsushi and Matsukura 2006). The fluid rich flow has been reported to be very effective in eroding the channel materials (Rickenmann et al. 2003). At this test site, the water content of channel bank sediments before erosion ranged from 5 to 8%, while it was 16% to 26% for debris surges in the channel (see Table 1). The water content in debris flow could also vary significantly in successive surges. The water-rich dilute debris flow surges effectively saturated the slope and bank sediments which were then eroded by angular rock fragments entrained in dense viscous surges. As a result, the sediments can be effectively removed and entrained by the debris flow, increasing the flow volume and subsequently boosting its destructive power (e.g. flow inundation area, height, velocity and runout distance) to the downstream regions (Iverson et al. 1998; Mangeney et al. 2010).

As stated in Huang et al. (2002), the real hillslope surface conditions (e.g., slope, roughness) vary significantly with the topographic position affecting the intensity of slope erosion and sediment production. Due to the limitations of site experiments, the complex slope topography was not studied. However, the configuration of the piled slope in the channel could mimic the local slope condition of a relatively smooth surface. Thus, the site experiments carried out in this work could clarify some general features of slope erosion by surges of debris flow in the channel.

Conclusions

In this research, slope erosion by surges of debris flow were investigated through field observations and experiments along an active natural debris flow gully. The major findings are summarized as follows:

1. The sediments in the alluvial slope were generally loose and unconsolidated, with the water content higher than 5%. The particle size distribution followed well the Weibull's cumulative distribution, with the mean value in the range of 2 ~ 4 mm. The particle shapes were primarily elongated or prismoidal and their aspect ratios followed well a normal distribution with the mean value of 0.4.
2. The dynamics of debris flow surges in the channel was controlled by the conditions of water and sediment supplies from the upstream reaches. During successive surges, the channel could quickly fill and expand through the entrainment of bed sediments and erosion of channel banks, which significantly changed the width and depth of the channel.
3. The combined effects of sediment saturation by water in dilute debris flow surges and abrasion by angular rock fragments entrained in dense viscous surges effectively increased the overall erosion intensity of debris flows. The backward erosion occurred on the downslope surface where the flow velocity was high. Due to its low strength and unconsolidated loose structure, the incised channel banks collapsed regularly adding the entrained sediment volume and increasing the channel width.
4. The clay slurry in debris flow exhibited a clear shear-thinning behavior, and its viscosity decreased with the increase of shear strain rate following well the power-law model. The flow had a low viscosity near the channel banks where high shear strain exists, while highly viscous flow maintained in the middle stream. Debris flow surges of high slurry viscosity and density can effectively transport a large portion of coarse gravels to downstream regions.

Data availability

All data generated during the study are available from the corresponding author by request.

Code availability

Not applicable.

Declarations

Ethics approval Not applicable.

Consent to participate Not applicable.

Consent for publication The authors declare that this is an original paper which has neither previously been published, nor under consideration for publication anywhere else; that its publication has been approved by all co-authors. All the data is authentic and was developed by the authors.

Conflict of interest The authors declare no competing interests.

References

AntonPaar (2021) Rheometer. Retrieved from https://www.anton-paar.com/corp-en/products/group/rheometer/

Berger C, McArdell BW, Schlunegger F (2011) Direct measurement of channel erosion by debris flows, Illgraben, Switzerland. J Geophys Res Earth Surf 116:F01002

Bird RB (1976) Useful non-Newtonian models. Annu Rev Fluid Mech 8(1):13–34

Ceylan K, Herdem S, Abbasov T (1999) A theoretical model for estimation of drag force in the flow of non-newtonian fluids around spherical solid particles. Powder Technol 103(3):286–291

Chen J, He YP, Wei FQ (2005) Debris flow erosion and deposition in Jiangjia Gully, Yunnan. China Environ Geol 48(6):771–777

Chhabra RP (2007) Bubbles, drops, and particles in non-Newtonian fluids (2nd ed.) CRC Press

Coe JA, Kinner DA, Godt JW (2008) Initiation conditions for debris flows generated by runoff at Chalk Cliffs, central Colorado. Geomorphology 96(3):270–297

Costa (1984) Physical Geomorphology of Debris Flows. In J. E. Costa, & P. J. Fleisher (Eds.), *Developments and Applications of Geomorphology* (pp. 268–317). Berlin, Heidelberg: Springer Berlin Heidelberg. Retrieved from https://doi.org/10.1007/978-3-642-69759-3_9

Crosta G (1998) Regionalization of rainfall thresholds: an aid to landslide hazard evaluation. Environ Geol 35(2):131–145

Crosta GB, Frattini P (2004) Controls on modern alluvial fan processes in the central Alps, northern Italy. Earth Surf Proc Land 29(3):267–293

Cui P, Zeng C, Lei Y (2015) Experimental analysis on the impact force of viscous debris flow. Earth Surf Proc Land 40(12):1644–1655

Davies TRH (1986) Large debris flows: A macro-viscous phenomenon. Acta Mech 63(1):161–178

Denlinger RP, Iverson RM (2001) Flow of variably fluidized granular masses across three-dimensional terrain: 2. Numerical predictions and experimental tests. Journal of Geophysical Research: Solid Earth 106:553–566

Egashira S, Honda N, Itoh T (2001) Experimental study on the entrainment of bed material into debris flow. Phys Chem Earth Part C 26(9):645–650

Guthrie RH, Hockin A, Colquhoun L, Nagy T, Evans SG, Ayles C (2010) An examination of controls on debris flow mobility: Evidence from coastal British Columbia. Geomorphology 114(4):601–613

Hu M, Wang R, Shen J (2011) Rainfall, landslide and debris flow intergrowth relationship in Jiangjia Ravine. J Mt Sci 8(4):603–610. https://doi.org/10.1007/s11629-011-2131-6

Huang C, Gascuel-Odoux C, Cros-Cayot S (2002) Hillslope topographic and hydrologic effects on overland flow and erosion. CATENA 46(2):177–188

Hungr O, Evans SG, Bovis MJ, Hutchinson JN (2001) A review of the classification of landslides of the flow type. Environ Eng Geosci 7(3):221–238

Hungr O, McDougall S, Bovis M (2005) Entrainment of material by debris flows. In M. Jakob, & O. Hungr (Eds.), *Debris-flow Hazards and Related Phenomena* (pp. 135–158). Berlin, Heidelberg: Springer Berlin Heidelberg. Retrieved from https://doi.org/10.1007/3-540-27129-5_7

Iverson RM, Reid ME, Logan M, LaHusen RG, Godt JW, Griswold JP (2011) Positive feedback and momentum growth during debris-flow entrainment of wet bed sediment. Nat Geosci 4(2):116–121

Iverson RM, Schilling SP, Vallance JW (1998) Objective delineation of lahar-inundation hazard zones. GSA Bull 110(8):972–984

Jakob M, Bovis M, Oden M (2005) The significance of channel recharge rates for estimating debris-flow magnitude and frequency. Earth Surf Proc Land 30(6):755–766

Loye A, Pedrazzini A, Theule JI, Jaboyedoff M, Liébault F, Metzger R (2012) Influence of bedrock structures on the spatial pattern of erosional landforms in small alpine catchments. Earth Surf Proc Land 37(13):1407–1423

Mangeney A, Roche O, Hungr O, Mangold N, Faccanoni G, Lucas A (2010) Erosion and mobility in granular collapse over sloping beds. J Geophys Res Earth Surf 115:F03040

Matsushi Y, Matsukura Y (2006) Cohesion of unsaturated residual soils as a function of volumetric water content. Bull Eng Geol Env 65(4):449

McCoy SW, Kean JW, Coe JA, Tucker GE, Staley DM, Wasklewicz TA (2012) Sediment entrainment by debris flows: In situ measurements from the headwaters of a steep catchment. J Geophys Res Earth Surf 117:F03016

Microtrac (2021) Dynamic Image Analysis. Retrieved from https://www.microtrac.com/products/particle-size-shape-analysis/dynamic-image-analysis/

Pierson TC (1980) Erosion and deposition by debris flows at Mt Thomas, North Canterbury, New Zealand. Earth Surface Processes 5(3):227–247

Rickenmann D, Weber D, Stepanov B (2003) Erosion by debris flows in field and laboratory experiments. Paper presented at the Debris-Flow Hazards Mitigation.Mechanics, Prediction, and Assessment. Proceedings of the Third International Conference on Debris-Flow Hazards Mitigation 2:883–894

Sauchyn DJ, Cruden DM, Hu XQ (1998) Structural control of the morphometry of open rock basins, Kananaskis region, Canadian Rocky Mountains. Geomorphology 22(3):313–324

Scott KM, Wang Y (2004) Debris flows: geologic process and hazard; illustrated by a surge sequence at Jiangjia Ravine, Yunnan, China. Reston, VA: Retrieved from USGS Publications Warehouse Retrieved from http://pubs.er.usgs.gov/publication/pp1671

Stock JD, Dietrich WE (2006) Erosion of steepland valleys by debris flows. GSA Bull 118(9–10):1125–1148

Stock JD, Schmidt KM, Miller DM (2008) Controls on alluvial fan longprofiles. GSA Bull 120(5–6):619–640

Theule JI, Liébault F, Laigle D, Loye A, Jaboyedoff M (2015) Channel scour and fill by debris flows and bedload transport. Geomorphology 243:92–105

Wang G, Sassa K, Fukuoka H (2003) Downslope volume enlargement of a debris slide–debris flow in the 1999 Hiroshima, Japan, rainstorm. Eng Geol 69(3):309–330

Wei H, Zhao T, Meng Q, Wang X, Zhang B (2020) Quantifying the morphology of calcareous sands by dynamic image analysis. Int J Geomech 20(4):04020020

Zhou GGD, Li S, Song D, Choi CE, Chen X (2019) Depositional mechanisms and morphology of debris flow: physical modelling. Landslides 16(2):315–332

Tao Zhao (✉)
Department of Civil and Environmental Engineering, Brunel University London, London UB8 3PH, UK
Email: tao.zhao@brunel.ac.uk

Gordon G. D. Zhou · Dongri Song
Institute of Mountain Hazards and Environment, Chinese Academy of Sciences, Chengdu, China

Qicheng Sun
State Key Laboratory of Hydroscience and Engineering, Tsinghua University, Beijing, China

Giovanni B. Crosta
Department of Earth and Environmental Sciences, Università Degli Studi Di Milano Bicocca, Piazza della Scienza 4, 20126 Milan, Italy